Flow instability criteria in processing map of superalloy GH79

ZHOU Ge[1], DING Hua[1], CAO Fu-rong[1], HAN Yin-ben[1], ZHANG Bei-jiang[2]

1. School of Materials and Metallurgy, Northeastern University, Shenyang 110819, China;

2. High Temperature Materials Division, Central Iron and Steel Research Institute, Beijing 100081, China

Abstract: Hot compression tests were conducted on a Gleeble−1500D thermal simulating tester. Based on the deformation behavior and microstructural evolution of superalloy GH79, different types of instability criteria of PRASAD, GEGEL, MALAS, MURTY and SEMIATIN were compared, and the physical significance of parameters was analyzed. Meanwhile, the processing maps with different instability criteria were obtained. It is shown that instability did not occur when average power dissipation rate was larger than 60% in the temperature range of 900−930 °C and 960−1080 °C, corresponding to the strain rate range of $5\times10^{-4}-1.8\times10^{-1}$ s^{-1} and $5\times10^{-4}-1.5\times10^{-1}$ s^{-1}, respectively. The two domains are appropriate for the processing deformation of superalloy GH79.
Key words: nickel-based superalloy; hot compression; flow instability criterion; processing map

1 Introduction

GH79 nickel-based high temperature alloy is a casting high temperature alloy. Its corresponding Russia brand is ЭК79, a modification of Russia ЭП742. Based on ЭП742 alloy, the contents of Al, Ti, Nb, and Mo are raised to more than 8.5% and meantime strengthening elements W and V are added to the as-cast GH79 alloy to form Ni−Cr−Co solid solution and Ni$_3$(Ti,Al,Nb) type γ' phase. Thus, this alloy possesses higher thermal strengthening properties and integrative properties, and long-term working stability and excellent service performance. Its service temperature is raised from 750 °C of ЭП742 alloy to 800 °C. At present, such nickel-based alloy has been used extensively to fabricate turbine discs of military and civil advanced engines in Russia [1].

Processing map is a powerful tool in the design and optimization of metallic forming process. It not only describes the deformation mechanisms of specific microstructures in deterministic regions but also describes the instability flow regions that should be avoided during forming process. In the meantime, optimized forming temperature and strain rates can be obtained by processing map. Therefore, the processing maps have been used in more than 200 alloys [2−7]. At present, most researchers only consider one instability criterion during the determination of working process. It is shown that the existing criteria for determining the "safe" and "unsafe" regions during hot working procedures are different in their theoretical basis, formula and physical significance, sometimes even contradictory. Some review articles about the plastic instability criteria can be found in many literatures. However, there is little information available about the workability analysis by combining other instability criterions.

In the present work, based on the concepts of dynamic material model (DMM) proposed by GEGEL [8], different instability criteria of PRASAD, GEGEL et al [9], MALAS and SEETHARAMAN [10], MURTY et al [11] and SEMIATIN and JONAS [12] are applied to studying the hot compression deformation of GH79 superalloy and valuable conclusions are derived by analyzing and comparing above instability criteria.

2 Experimental

The chemical composition (mass fraction, %) of the GH79 superalloy in this investigation was as follows: 0.061 C, 11.15 Cr, 14.26 Co, 2.41 W, 4.51 Mo, 3.10 Al, 2.75 Ti, 2.75 Nb, 0.61 V, 0.56 Fe, 0.045 Si, 0.002 La, 0.005 Ce, 0.0009 S, 0.005 P and balance Ni. Hot compression tests were performed on a Gleeble−1500D

thermal-force simulation testing machine for GH79 superalloy specimen whose dimensions were d8 mm×12 mm. The test temperature was in the range of 900−1150 °C with a temperature interval of 50 °C. The strain rate was in the range of $5×10^{-4}$−10 s^{-1}, the heating velocity was 10 °C/s and holding time was 3 min. Then the specimens were deformed to a true strain of 0.6 and the specimens were immediately water-cooled to room temperature after deformation ended.

The deformed specimens were sectioned parallel to the compression direction and the cutting surfaces, polished with emery papers up to 1000#, and cleaned with acetone to remove grease for microstructure observation. The metallographic specimens were etched using a solution of $CuSO_4$ (1.5 g) + HCl (40 mL) + C_2H_5OH (20 mL). The microstructures of the specimens were investigated by optical microscopy (OM) using an OLYMPUS GX51 microscope.

3 Results and discussion

3.1 Processing map theory based on DMM

According to the theory of dissipative structures, PRASAD [13] believed that the energy of input system, P, can be divided into dissipative magnitude, G, and dissipative coordination magnitude, J. Its mathematical definition is

$$P = \sigma\dot{\varepsilon} = G + J = \int_0^{\dot{\varepsilon}} \sigma d\dot{\varepsilon} + \int_0^{\sigma} \dot{\varepsilon} d\sigma \tag{1}$$

where G is the energy consumed by the plastic deformation of materials among which a majority of energy is turned into thermal energy and small amount of energy is stored in crystal defect energy; J is the energy dissipated during the microstructure evolution of material deformation. The proportion of two energies is determined by the strain rate sensitivity exponent, m, of forming component under definite stress:

$$m = \partial J / \partial G = \dot{\varepsilon}\partial\sigma / \sigma\partial\dot{\varepsilon} = \partial\ln\sigma / \partial\ln\dot{\varepsilon} \tag{2}$$

The physical meaning of partition rate of system energy can be elucidated clearly from the viewpoint of atomic movement. The dissipation of material energy can be divided into potential energy and kinetic energy. Potential energy is related to the relative positions among atoms. The variation of microstructure will result in the variation of atomic potential energy and hence corresponds to the dissipative coordination magnitude, J. Kinetic energy is related to the movement of atoms, i.e., the movement of dislocations. Kinetic energy conversion is dissipated in the form of thermal energy and hence corresponds to dissipative magnitude, G. Differential calculus of dissipative coordination magnitude J is expressed as:

$$dJ = \dot{\varepsilon}d\sigma \tag{3}$$

Presuming that material conforms to constitutive relationship:

$$\sigma = C\dot{\varepsilon}^m \tag{4}$$

Then, J is expressed as:

$$J = \int_0^{\dot{\varepsilon}} \sigma d\dot{\varepsilon} = m/(m+1)\sigma\dot{\varepsilon} \tag{5}$$

When $m=1$, material is in an ideal linear dissipation state. Dissipative coordination magnitude J reaches the maximum value J_{max}, i.e.,

$$J_{max} = \sigma\dot{\varepsilon} / 2 \tag{6}$$

A dimensionless parameter value η which is the power dissipation rate can be obtained by Eqs. (5) and (6). Its physical meaning is to elucidate the proportion relation of energy dissipated by microstructure evolution to linear dissipation energy during material forming. Its value is:

$$\eta = J / J_{max} = 2m(m+1) \tag{7}$$

The flow stresses at different strain rates and temperatures with a strain of 0.6 were obtained by thermal simulation compression test and the power dissipation map was obtained, as shown in Fig. 1.
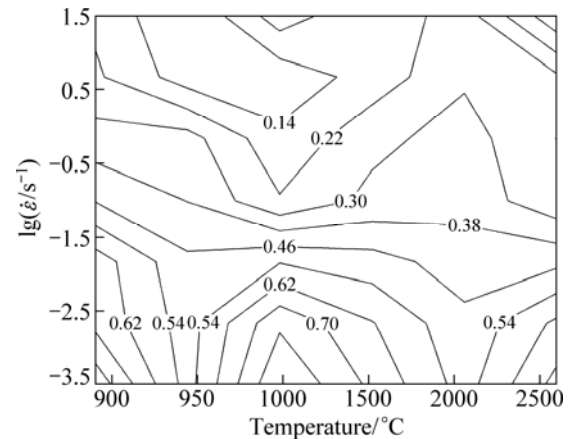
Fig. 1 Power dissipation rate map at different strain rates and temperatures with a strain of 0.6

It can be seen from Fig. 1 that when hot forming is performed in region I (temperature of 900−930 °C and strain rate of $5×10^{-4}$−$1.8×10^{-1}$ s^{-1}), region II (temperature of 960−1080 °C and strain rate of $5×10^{-4}$−$1.5×10^{-1}$ s^{-1}), the mean value of power dissipation rate of GH79 superalloy is 62%. The maximum value is 70%.

3.2 Analysis and application of different instability criteria for GH79 superalloy

3.2.1 GEGEL's instability criterion

Based on the second law of thermodynamics, GEGEL [8] found that flow instability is related to the temperature sensitivity parameter, s. The definition of s is as follows:

$$s = (1/T)(\partial \ln \sigma / \partial (1/T)) = -\partial \ln \sigma / \partial \ln T \tag{8}$$

Meanwhile, GEGEL used Lyaponov function $L(\eta,s)$ and believed that the flow stress curve is up-convex when stable flow occurs in the material. Flow stress decreases with increasing temperature. η decreases with increasing $\dot{\varepsilon}$. s decreases with increasing $\dot{\varepsilon}$.

$$\partial s / \partial \ln \dot{\varepsilon} = -\partial (\partial \ln \sigma) / ((\partial \ln T)(\partial \ln \dot{\varepsilon}))$$
$$= -\partial m / \partial \ln T > 0 \Rightarrow \partial m / \partial \ln T < 0 \tag{9}$$

Thus, GEGEL's instability criterion becomes:

$$\partial \eta / \partial \ln \dot{\varepsilon} > 0, \ \partial m / \partial \ln T < 0 \tag{10}$$

The processing map on GEGEL's instability criterion of the GH79 superalloy generated at a strain of 0.6 is shown in Fig. 2. The map is clearly classified into two domains, e.g., the stability deformation domain, and the instability deformation domain. The latter is shaded in Fig. 2. GEGEL's criterion is derived on the basis of thermodynamics theorem and its theoretical basis is strict.
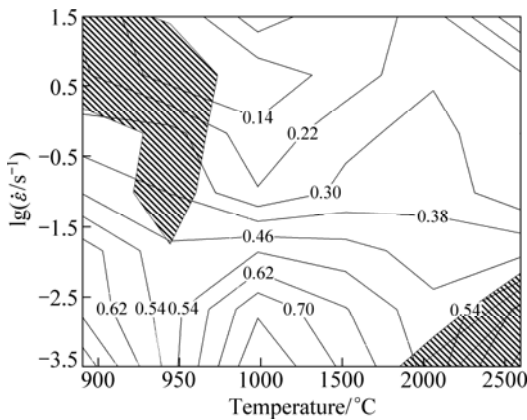

Fig. 2 Processing map of GEGEL's instability criterion for GH79 superalloy

3.2.2 MALAS's instability criterion

When MALAS and SEETHARAMAN [10] investigated Ti−49.5Al− 2.5Nb−1.1Mn alloy, they used Lyaponov function $L(\eta,s)$ and meantime replaced η with m. They proposed MALAS's instability criterion on the basis of GEGEL's criterion:

$$\partial m / \partial \ln \dot{\varepsilon} > 0, \ \partial m / \partial \ln T < 0 \tag{11}$$

The processing map on MALAS's instability criterion of the GH79 superalloy generated at the strain of 0.6 is shown in Fig. 3.

MALAS's criterion was obtained by replacing η with m on the basis of GEGEL's criterion. It can be seen
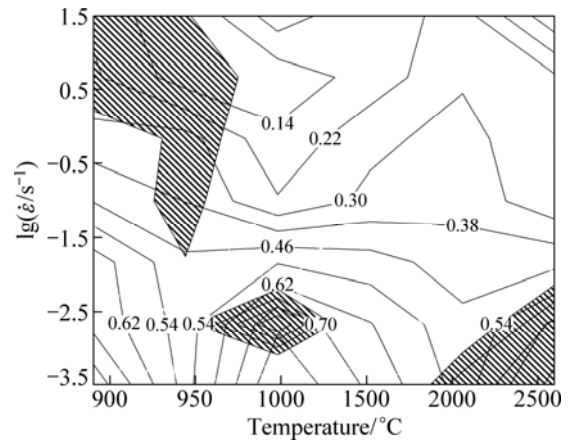

Fig. 3 Processing map of MALAS's instability criterion for GH79 superalloy

from Fig. 2 and Fig. 3 that the instability domains of these two instability criteria are basically the same. However, as compared with the requirements of GEGEL's criterion that m value is a constant, MALAS's criterion needs not consider m value as a constant. Therefore, MALAS's criterion is more expansive than GEGEL's criterion.

3.2.3 PRASAD's instability criterion

At present, when DMM method is used to solve hot working problem, GEGEL's and MALAS's instability criteria have been rarely used. Many scholars used the instability criterion established by PRASAD and SESHACHRYULU [14]. This kind of criterion takes the extremum principle of irreversible thermodynamics of large plastic flow and satisfies following relation when flow instability occurs:

$$\partial D / \partial R < D / R \tag{12}$$

As dissipation coordination magnitude is relevant to the microstructure evolution of metallurgical process, PRASAD et al replaced D with J and got:

$$\partial J / \partial \dot{\varepsilon} < J / \dot{\varepsilon} \tag{13}$$

$$\partial \ln J / \partial \ln \dot{\varepsilon} < 1 \tag{14}$$

Taking logarithm on both sides of Eq. (5) and seeking local derivation for $\ln \dot{\varepsilon}$, one gets:

$$\partial \ln J / \partial \ln \dot{\varepsilon} =$$
$$\partial \ln[m/(m+1)] / \partial \ln \dot{\varepsilon} + \partial \ln \sigma / \partial \ln \dot{\varepsilon} + 1 \tag{15}$$

Integrating Eqs. (5), (14) and (15), one gets PRASAD's instability criterion:

$$\xi(\dot{\varepsilon}) = \partial \ln[m/(m+1)] / \partial \ln \dot{\varepsilon} + m < 0 \tag{16}$$

The processing map on PRASAD's instability criterion of the GH79 superalloy generated at the strain of 0.6 is shown in Fig. 4.

PRASAD's criterion is derived carefully by the maximum entropy generation rate principle and large plastic deformation, as compared with other criteria, the scope of instability region is the smallest, as shown in Fig. 4.
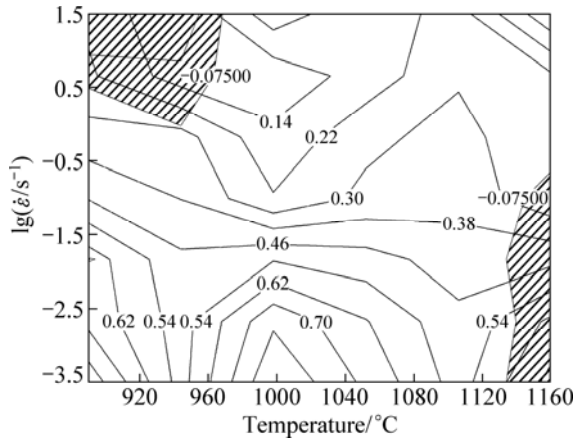
Fig. 4 Processing map of PRASAD's instability criterion for GH79 superalloy

3.2.4 MURTY's instability criterion

It is believed that m value in Eq. (4) of PRASAD's criterion is constant. But MURTY et al [15−20] and SPIGARELLI et al [21] believed that for pure metal and alloy with low alloying elements, m could be considered simply a constant value; while m is not constant for complex alloy system. Based on this situation, MURTY et al [15] derived a instability region criterion that is suitable for any stress and strain rate curve. According to the definition of J and η:

$$J = \int_0^\sigma \dot{\varepsilon}\,\mathrm{d}\sigma \Rightarrow \partial J / \partial \dot{\varepsilon} = \dot{\varepsilon} \cdot \partial \sigma / \partial \dot{\varepsilon}$$
$$= \sigma \cdot \partial \ln \sigma / \partial \ln \dot{\varepsilon} = m\sigma \tag{17}$$

$$\eta = J / J_{\max} = 2J / (\sigma \dot{\varepsilon}) \Rightarrow J / \dot{\varepsilon} = \eta \sigma / 2 \tag{18}$$

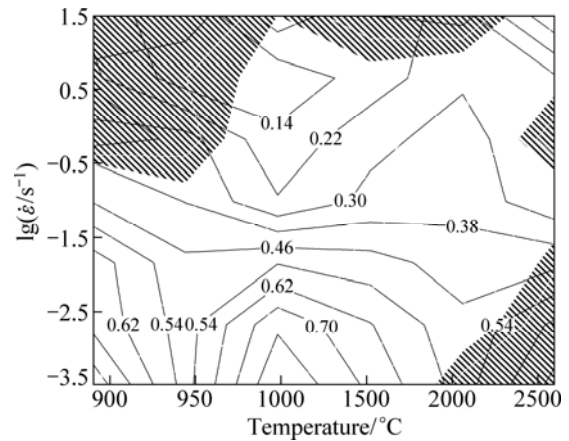and Eq. (13), one gets MURTY's instability criterion:

$$2m < \eta \tag{19}$$

The processing map on MURTY's instability criterion of the GH79 superalloy generated at the strain of 0.6 is shown in Fig. 5.

Entire derivation process of MURTY's criterion does not involve the problem that whether or not m value is a constant, and the application scope of this criterion is the most expansive. However, during calculating η value, the definition formula of η value must be used to solve and the calculation process is cockamamie.

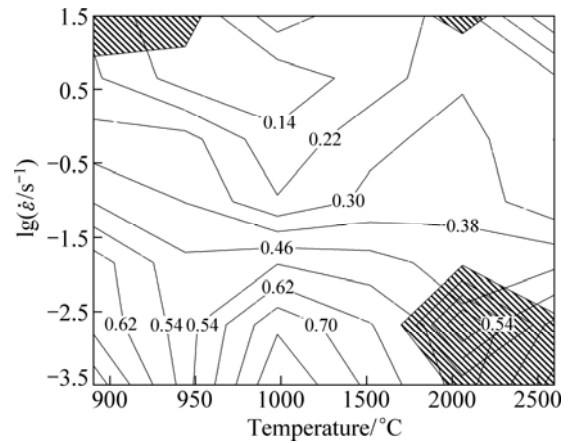### 3.2.5 SEMIATIN's instability criterion

SEMIATIN and JONAS [12] put forwards the relationship of flow softening with material parameter α, $\alpha = -\gamma/m$, where γ is flow softening rate, $\gamma = \partial(\ln\sigma)/\partial\varepsilon$. The SEMIATIN's flow localization criterion becomes:

Fig. 5 Processing map of MURTY's instability criterion for GH79 superalloy

$$\alpha > 5 \tag{20}$$

The processing map on SEMIATIN's instability criterion of the GH79 superalloy generated at the strain of 0.6 is shown in Fig. 6.

Fig. 6 Processing map of SEMIATIN's instability criterion for GH79 superalloy

SEMIATIN's criterion is an empirical formula derived on the basis of microstructure observation of titanium and its alloys. But as compared with other several criteria, this criterion does not take strict theory derivation as the basis, thus its scope of application is restricted greatly.

3.3 Analysis of hot forming properties for GH79 superalloy

The processing map on different instability criteria of the GH79 superalloy generated at the strain of 0.6 is shown in Fig. 7.

Five regions of I, II, III, IV and V in Fig. 7 represent the flow instability domains under five different instability criteria of GEGEL, MALAS, PRASAD, MURTY and SEMIATIN, respectively. It can be seen

from Fig. 7 that the superposition of five flow instability criteria appears in top left corner and low right corner domains which are in the temperature range of 900−950 °C over a strain rate range of 1−10 s^{-1}, and in the temperature range of 1100−1150 °C over a strain rate range of 5×10^{-4}−5×10^{-2} s^{-1}, indicating that working instability phenomenon appears in above forming domains and should be avoided during practical forming process. Flow instability phenomenon probably appears in the instability domains with less superposition of flow instability criteria. The domains with high power dissipation rate and no flow instability are appropriate for the forming.
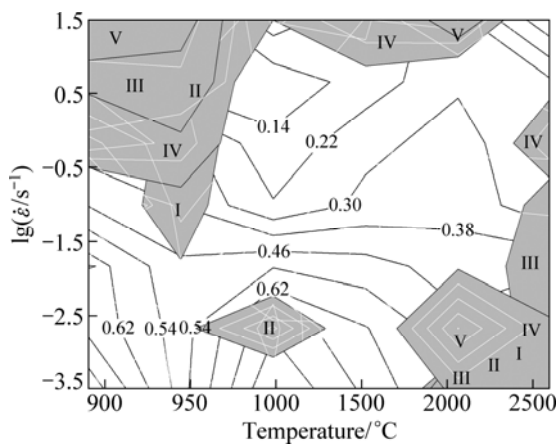

Fig. 7 Instability maps through different instability criteria for GH79 superalloy: I—GEGEL; II—MALAS; III—PRASAD; IV—MURTY; V—SEMIATIN

It can be seen from Fig. 7 that the instability domains obtained by different instability criteria are different. Intersection and supplement occur among the instability domains. Therefore, when hot forming workability of GH79 superalloy is analyzed, different instability criteria should be considered integratively. The instability domains of hot forming can be judged correctively using integrative criterion.

GEGEL's criterion is derived on the basis of thermodynamics theorem and its theoretical basis is strict. MALAS's criterion is obtained by replacing η with m on the basis of GEGEL's criterion. It can be seen from Fig. 7 that the instability regions of these two instability criteria are basically the same. However, as compared with the requirements of GEGEL's criterion that m value is a constant parameter, MALAS's criterion needs not consider m value as a constant. Therefore, MALAS's criterion is more expensive than GEGEL's criterion. PRASAD's criterion is derived carefully by the maximum entropy generation rate principle and large plastic deformation, as compared with other criteria, and the scope of instability region is the smallest, as shown in Fig. 7. Entire derivation process of MURTY's criterion

does not involve the problem that whether or not m value is a constant, so the application scope of this criterion is the most expansive. However, during calculating η value, the definition formula of η value must be used to solve and the calculation process is cockamamie. SEMIATIN's criterion is an empirical formula derived on the basis of microstructure observation of titanium and its alloys. But as compared with other several criteria, this criterion does not take strict theory derivation as the basis, thus its scope of application is restricted greatly.

The microstructural evolution during deformation is shown in Fig. 8. Figure 8(a) shows the metallograph at a temperature of 1150 °C and a strain rate of 10^{-3} s^{-1}. It can be seen that obvious cavitations and cracks appear between phases γ and γ', indicating that flow instability will appear at cavitations and cracks during deformation. Figure 8(b) shows the metallograph at a temperature of 900 °C and at a strain rate of 10^{-1} s^{-1}. It can be seen that cavitations and cracks appear at triple junction grain
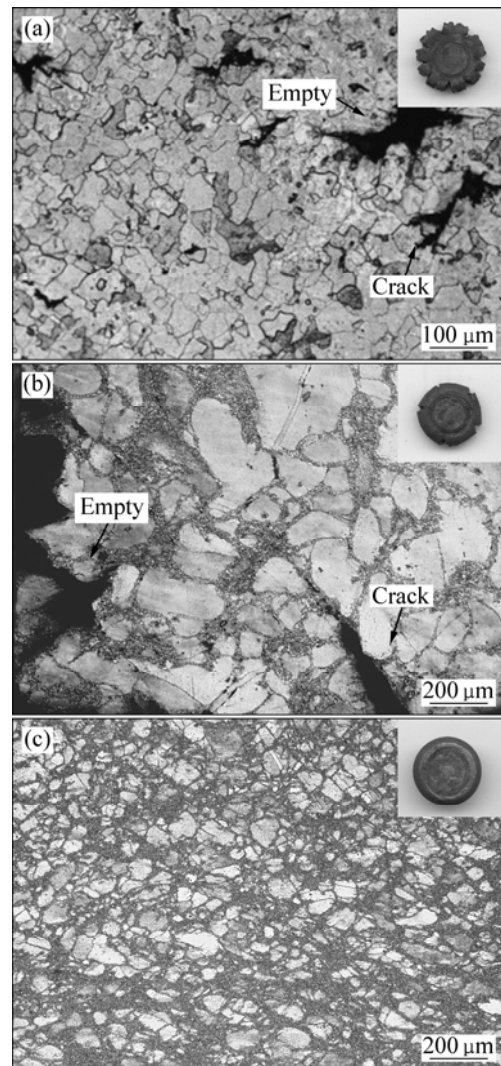
Fig. 8 Microstructures of deformed specimens in different domains: (a) $\dot{\varepsilon}$=10^{-3} s^{-1}, t=1150 °C; (b) $\dot{\varepsilon}$=10^{-1} s^{-1}, t=900 °C; (c) $\dot{\varepsilon}$=10^{-1} s^{-1}, t=1050 °C

boundaries. The reason is that when deformation temperature is low and strain rate is high, it is difficult for grains at grain boundary to slide during deformation. Thus, stress concentration is formed at triple junction grain boundary. Dynamic recrystallization cannot proceed fully at 900 °C, and hence the stress concentration formed at triple junction grain boundary cannot be relaxed under high strain rate. Therefore, cavitations and cracks at triple junction grain boundary appear under high strain rate and hence flow instability appears. Figure 8(c) shows the metallograph at a temperature of 1050 °C and a strain rate of 10^{-1} s^{-1}. It can be seen that fine equiaxed grains exist and dynamic recrystallization occurs under this condition. The progression of dynamic recrystallization relaxes the stress concentration effectively at triple junction grain boundary. Thus, GH79 alloy has excellent hot forming performance under this deformation condition.

4 Conclusions

1) According to power dissipation rate maps integrating several different instability criteria, appropriate forming domains of GH79 superalloy are in the temperature range of 900−930 °C and strain rate range of 5×10^{-4}−1.8×10^{-1} s^{-1} and in the temperature range of 980−1030 °C and strain rate range of 5×10^{-4}−1.5×10^{-1} s^{-1}.

2) Flow instability phenomenon appears in low temperature and high strain rate domain and high temperature and low strain rate domain for forming GH79. The reason is that cavitations and cracks appear due to the stress concentration at triple junction grain boundary and excessive high temperature. Dynamic recrystallization takes place in appropriate domains and relaxes the stress concentration at triple junction grain boundary. Thus the alloy has excellent forming performance in this region.

3) Analysis and comparison of different instability criteria of GH79 superalloy revealed that the instability domains of this alloy under different instability criteria are different. The flow instability predicted by PRASAD's criterion and MURTY's criterion are more effective at high strain rate, which are the preferential choices in most cases. GEGEL's criterion and MALAS's criterion can predict the flow instability at high temperature and low strain rate. However, further study for validation by experiment is required.

References

[1] HUANG Fu-xiang. Development of turbine disk high superalloys in Russia [J]. Journal of Aeronautical Materials, 1993, 13(4): 49−56.

[2] SUN Yu, ZENG Wei-dong, ZHAO Yong-qing, ZHANG Xue-min, MA Xiong, HAN Yuan-fei. Constructing processing map of Ti40 alloy using artificial neural network [J]. Transactions of Nonferrous Metals Society of China, 2011, 21(1): 159−165.

[3] HUANG Shu-hai, ZHAO Zu-de, XIA Zhi-xin, CAI Hai-yan, KANG Feng, HU Chuan-kai, SHU Da-yu. Study on high-temperature deformation behavior and processing map of AZ80 alloy [J]. Rare Metal Materials and Engineering, 2010, 39(5): 848−852. (in Chinese)

[4] YAN Liang-ming, SHEN Jian, LI Zhou-bing, LI Jun-peng, YAN Xiao-dong, MAO Bai-ping. Modelling for flow stress and processing map of 7055 aluminum alloy based on artificial neural networks [J]. The Chinese Journal of Nonferrous Metals, 2010, 20(7): 1296−1301. (in Chinese)

[5] ZENG Li-ying, YANG Guan-jun, GE Peng, MAO Xiao-nan, ZHAO Yong-qing, ZHOU Lian. Processing map of one kind of metastable β titanium alloy [J]. Rare Metal Materials and Engineering, 2010, 39(9): 1505−1508. (in Chinese)

[6] LI Liang, SONG De-jun. Microstructure and processing map of hot compressing deformation of Ti80 alloy [J]. The Chinese Journal of Nonferrous Metals, 2010, 20(10): 738−742. (in Chinese)

[7] KONG Fan-tao, ZHANG Shu-zhi, CHEN Yu-yong. Hot deformation and processing map of Ti−46Al−2Cr−4Nb−Y alloy [J]. The Chinese Journal of Nonferrous Metals, 2010, 20(10): 233−236. (in Chinese)

[8] GEGEL H L. Synthesis of atomistics and continuum modeling to describe microstructure: Computer simulation in material science [M]. OH: ASM, 1984: 291−344.

[9] GEGEL H L, MALAS J C, DORAIVELU S M, SHENDE V A. Modeling techniques used in forging process design Metals Handbook [M]. OH: ASM, 1984: 219−344.

[10] MALAS J C, SEETHARAMAN V. Using material behavior models to develop process control strategies [J]. JOM, 1992, 6: 8−14.

[11] MURTY NARAYANA S V S, NAGESWARRA RAO B, KASHYAP B P. Instability criteria for hot deformation of materials [J]. International Materials Reviews, 2000, 45(1): 15−26.

[12] SEMIATIN S L, JONAS J J. Formability and workability of metals: Plastic instability and flow localization [M]. Metal Park, OH: ASM International, 1984: 51−78.

[13] PRASAD Y V R K. Recent advances in the science of mechanical processing [J]. Indian J Technol, 1990, 4: 435−451.

[14] PRASAD Y V R K, SESHACHRYULU T. Modelling of hot deformation for microstructural contral [J]. International Materials Reviews, 1988, 43(6): 243−252.

[15] MURTY S V S N, RAO B N. On the development of instability criteria during hotworking with reference to IN 718 [J]. Mater Sci Eng A, 1998, 254(15): 76−82.

[16] MURTY S V S N, RAO B N. On the dynamic material model for the hot deformation of materials [J]. Journal of Materials Science Letters, 1999, 18(21): 1757−1758.

[17] MURTY S V S N, RAO B N. On the flow localization concept in the processing maps of titanium alloy Ti−24Al−20Nb [J]. Journal of Materials Processing Technology, 2000, 104(15): 103−109.

[18] MURTY S V S N, RAO B N. On the hot working characteristics of INCONEL alloy MA754 using processing maps [J]. Scandinavian Journal of Metallurgy, 2000, 29(4): 146−150.

[19] MURTY S V S N, RAO B N, KASHYAP B P. On the hot working characteristics of 6061Al−SiC and 6061-Al_2O_3 particulate reinforced metalmatrix composites [J]. Composites Science and Technology, 2003, 63(1): 119−135.

[20] MURTY S V S N, RAO B N, KASHYAP B P. Development and validation of a processing map for AFNOR 7020 aluminium alloy [J]. Materials Science and Technology, 2004, 20(6): 772−782.

[21] SPIGARELLI S, CERRI E, CAVALIERE P, EVANGELISTA E. An analysis of hot formability of the 6061+20%Al_2O_3 composite by means of different stability criteria [J]. Mater Sci Eng A, 2002, 327(2): 144−154.

GH79 合金加工图的流变失稳准则

周 舸 [1]，丁 桦 [1]，曹富荣 [1]，韩寅奔 [1]，张北江 [2]

1. 东北大学 材料与冶金学院，沈阳 110819；
2. 钢铁研究总院 高温材料研究所，北京 100081

摘　要：在 Gleeble−1500D 热模拟实验机上对 GH79 合金进行热压缩模拟实验。在对于 GH79 合金热变形行为及微观组织演变研究的基础上，分析比较 Prasad, Gegel, Malas, Murty 和 Semiatin 5 种不同失稳判据，并绘制不同失稳判据的热加工图。从不同失稳判据的热加工图中可以看出，在温度 900~930 °C、应变速率 $5 \times 10^{-4} \sim 1.8 \times 10^{-1} \, s^{-1}$ 和温度 960~1080 °C、应变速率为 $5 \times 10^{-4} \sim 1.5 \times 10^{-1} \, s^{-1}$ 的两个范围内该合金的功率耗散率值大于 60%，上述两个区域为 GH79 合金的适合成形区域。

关键词：镍基高温合金；热压缩变形；流变失稳准则；加工图

(Edited by YANG Hua)